

# Current sheet structure near magnetic X-line observed by Cluster

A. Runov<sup>1</sup>, R. Nakamura<sup>1</sup>, W. Baumjohann<sup>1</sup>, R. A. Treumann<sup>2</sup>, T. L. Zhang<sup>1</sup>,  
M. Volwerk<sup>1</sup>, Z. Vörös<sup>1</sup>, A. Balogh<sup>3</sup>, K.-H. Glaßmeier<sup>4</sup>, B. Klecker<sup>2</sup>, H. Rème<sup>5</sup>, L. Kistler<sup>6</sup>

**Abstract.** In this paper we study Cluster observations during the interval 0947 - 0951 UT on 1 October 2001, when Cluster was located at  $X_{GSM} = 16.4 R_E$  near  $Z_{GSM} = 0$  in the pre-midnight magnetotail. During this interval the Cluster barycenter crosses the neutral sheet four times. High speed proton flow, with reversal from tailward to Earthward, was detected during the crossings. Using a linear gradient/curl estimator technique we estimate the current density and the magnetic field curvature within the crossings. The observations exhibit the tailward passage of an X-line over the Cluster tetrahedron. The current sheet has a bifurcated structure in the regions of tailward and earthward flows and a flat and/or slightly bifurcated thin current sheet in between. A distinct quadrupolar Hall magnetic field component was observed.

## 1. Introduction

Detection of a reconnection region and studying its current/plasma sheet structure is difficult using single spacecraft measurements. Cluster, being a four spacecraft constellation, offers a possibility to study the spatial structure of the plasma sheet near and/or within the reconnection region.

The standard macroscopic picture of magnetic reconnection includes an X-type magnetic neutral line, cold plasma inflow toward the neutral line and high speed accelerated plasma outflow. The outflow region is bounded by branches of a bifurcated current sheet. In the vicinity of the X-line the ideal MHD conditions are not valid. This scheme is supported by numerous MHD simulations [e.g. Ugai and Tsuda, 1977; Sato and Hayashi, 1979; Scholer, 1989] and analytical solutions [e.g. Semenov et al., 1998].

As it was proposed by Sonnerup [1979], ions and electrons move differently around the X-line, and this decoupling results in a Hall current system near the X-line. Terasawa [1983] found the Hall component of the magnetic field in a tearing mode stability analysis. It was also shown in Hall-MHD [e.g., Lottermoser and Scholer, 1997], hybrid [e.g., Lottermoser et al., 1998; Nakamura et al., 1998] and particle-in-cell [Hesse et al., 2001; Pritchett, 2001] simulations that a magnetic reconnection produces a quadrupolar out-of-plane component of the magnetic field. This out-of-plane field appears as a result of different motions of inflowing electrons and ions around the X-line. Its characteristic scale is of the order of

the ion inertial length. Measurements on-board the Geotail [Nagai et al., 2001] at  $X \sim 25\text{--}30 R_E$  and Wind [Øieroset et al., 2001] ( $X \sim 60 R_E$ ) showed the quadrupolar Hall magnetic field near the magnetic reconnection region. But it was not possible to estimate the characteristic scales of the Hall region using single spacecraft measurements. Asano [2001] studied the current sheet structure and non-MHD effects near an X-line using the statistical analysis of Geotail data. He found that the current sheet thickness in the vicinity of the X-line is about 500 km, and this thin current sheet (TCS) has a bifurcated structure with current density maxima for  $0.8 < b_x < 0.4$ , where  $b_x$  is normalized to the  $B_x$  in the lobe.

The purpose of this paper is to present multi-point observations of the magnetic reconnection region, detected by Cluster on 1 October 2001. Four-point measurements allow analyzing the current sheet structure in the reconnection region and estimating the characteristic scales for different parts of this region.

## 2. Observations and data analysis

At 0947-0951 UT on 1 October 2001, Cluster was located at  $[-16.4; +8; 0.5] R_E$ , (GSM coordinates are used). The Cluster tetrahedron configuration is shown in Figure 1 a,b. During a half-hour long interval 0930 - 1000 UT, Cluster repeatedly crosses the neutral sheet, located approximately in the  $Z_{GSM} = 0$  plane. The Cluster/FGM [Balogh et al., 2001] 1-s resolution data for 0947 - 0951 UT are shown in Figure 1 c,d. It is seen from FGM data and from the relative Cluster positions that during 0947 - 0951 UT  $B_x$  from s/c 1 is larger than  $B_x$  from the more southern s/c. Except for a short-time perturbation at  $\sim 0947:40\text{--}0947:45$  UT, the southernmost s/c 3 detects the smallest  $B_x$ . The magnetic field gradient is thus mainly directed along  $Z_{GSM}$ , and the GSM system is suitable for studying this event.

Data from the Cluster/CIS experiment [Rème et al., 2001] in the time interval 0947-0951 UT show a reversal of the proton bulk flow from tailward to earthward. Figure 1 e,f show the  $X_{GSM}$  and  $Z_{GSM}$  components of the perpendicular velocity vector  $\mathbf{V}_{\perp p} = \mathbf{b} \times (\mathbf{V}_p \times \mathbf{b})$ , where  $\mathbf{b} = \mathbf{B}/|B|$ , and  $\mathbf{V}_p$  is proton bulk velocity from CIS/CODIF. Spin-averaged ( $\sim 4$ , s) resolution data are used. Maximum (minimum) proton bulk velocity value from s/c 1, 3, 4 are  $\sim 900$  ( $\sim 700$ )  $\text{km s}^{-1}$  for the Earthward and tailward flows, respectively, which is  $\sim 0.5 V_A$ , with  $V_A$  the Alfvén speed in the lobe ( $B \sim 25$  nT,  $N_p \sim 0.1 \text{ cm}^{-3}$ , according to Cluster 1).

During the interval 0947-0951 UT Cluster 2, 3, 4 cross the neutral sheet four times. Cluster 1 stays in the northern hemisphere (NH) in close vicinity of the neutral sheet. During the first crossing (denoted as "A") Cluster 2, 3 and 4 traverse the neutral sheet from NH into the southern hemisphere (SH). They detect fast tailward proton bulk flows which are concentrated near  $B_x \sim 0$ . The value of  $B_z$  measured by s/c 2, 3 and 4 during crossing A are mostly negative with minima of -9, -22, -13 nT, respectively.

During the next crossing, marked "B", s/c 2, 3 and 4 return from SH to NH. It is clearly seen from the  $B_x$  traces of the spacecraft that the current sheet thins out during the traversal from A to B. During interval B, the X-component of  $\mathbf{V}_{\perp}$  is about zero. Cluster 1,

<sup>1</sup>Institut für Weltraumforschung der ÖAW, Graz, Austria.

<sup>2</sup>Max-Planck-Institut für extraterrestrische Physik, Garching, Germany.

<sup>3</sup>Imperial College, London, UK.

<sup>4</sup>TU Braunschweig, Braunschweig, Germany.

<sup>5</sup>CESR/CNRS, Toulouse, France.

<sup>6</sup>University of New Hampshire, Durham, NH, USA

staying in NH, detects a negative  $Z$  component  $V_{\perp z}$ , while s/c 4 in SH sees a positive  $V_{\perp z}$  in between  $A$  and  $B$ . The  $B_z$  components at s/c 1, 2, and 4 are about zero. In contrast,  $B_z \sim 5$  nT at s/c 3 with a peak value of 16 nT at 0948:50 UT.

During the interval  $C$  all four Cluster spacecraft cross the neutral sheet from NH to SH and detect fast Earthward proton bulk flows, focused at  $B_x \sim 0$ . The  $B_z$ -components are all positive with the tendency to grow. The maximum value of  $B_z$  is  $\sim 5$  nT. The  $Z$ -component of the proton bulk velocity s/c 1 and 4 changes from a negative in NH to a positive value in SH. The next SH  $\rightarrow$  NH crossing ( $D$ ) is characterized by a large positive  $V_{\perp x}$  and significant negative  $V_{\perp z}$ , and  $B_z \sim 5$ –8 nT.

According to the Kyoto quick look  $AE$  monitor (not shown) the magnetic activity during 1 October 2001 was high. The selected interval corresponds to a local peak of  $AE \sim 1000$  nT.

The correlation between the magnetic field measurements of the four spacecraft was high (correlation coefficient  $0.82 < R < 0.95$ ). Hence all spacecraft stay in the same physical region, and the linear gradient and curl estimator technique [Chanteur, 1998] can be applied. Figure 2 shows the magnetic field components in the tetrahedron barycenter (upper panel), the  $\text{curl } \mathbf{B}$  components,  $X$  and  $Y$  GSM components of the magnetic field curvature vector

$\text{curl } \mathbf{B} = (\mathbf{b} \cdot \nabla)\mathbf{b}$ , magnetic field divergence  $\text{div } \mathbf{B}$ , and  $X$ - and  $Z$ -components of the bulk proton flow from the mean value of the s/c 1, 3 and 4 CIS/CODIF measurements. The  $y$ -component of the current density  $\text{curl } \mathbf{B}$  has a maximum value of  $\sim 16$ –20 nT/10<sup>3</sup> km ( $j_y \sim 12$ –15 nA m<sup>-2</sup>) in the transition region between the tailward and earthward flow regions. There are significant peaks of in-plane ( $X$  and  $Z$ ) components of the  $\text{curl } \mathbf{B}$  over crossings  $A$  and  $B$ , which may be interpreted as Hall-current branches: positive  $X$ - and negative  $Z$ -components in the NH  $\rightarrow$  SH crossing during tailward flow ( $A$ ) and negative  $X$ , and weak positive  $Z$  components of the current density in the crossings  $C$  and  $D$  associated with strong earthward ion flow (see the schematic representation of the Hall current system by Nagai *et al.* [2001]). It should be noted that  $\text{div } \mathbf{B}$ , which is a measure of the accuracy of the calculation, ranges between  $\pm 5$  nT/10<sup>3</sup> km, except for a peak up to  $-10$  nT/10<sup>3</sup> km at 0948:40 UT.

The  $X$ -component of the magnetic field curvature dominates all four neutral sheet crossings. Moreover, the tailward flow ( $A$ ) is associated with a large negative  $X$ -component in the magnetic field curvature, while during the crossings  $B$ ,  $C$  and  $D$  the  $X$ -component of the curvature is positive. Thus, the magnetic field loop associated with tailward proton flow is open in the tailward direction, and the loop associated with earthward flow is open toward Earth. These

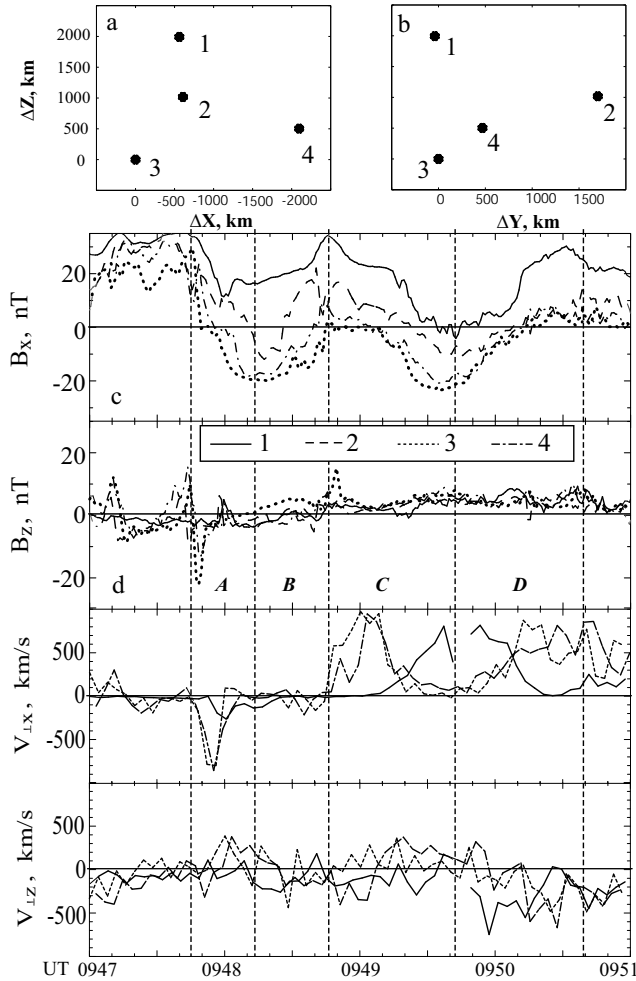


**Figure 1.** Cluster tetrahedron configuration (a,b) and measurements:  $X_{GSM}$  (c) and  $Z_{GSM}$  (d) components of the magnetic field from Cluster/FGM, 1-s resolution,  $X_{GSM}$  (e) and  $Z_{GSM}$  (f) components of perpendicular proton bulk velocity vector from Cluster/CIS-CODIF, spin resolution, versus UT

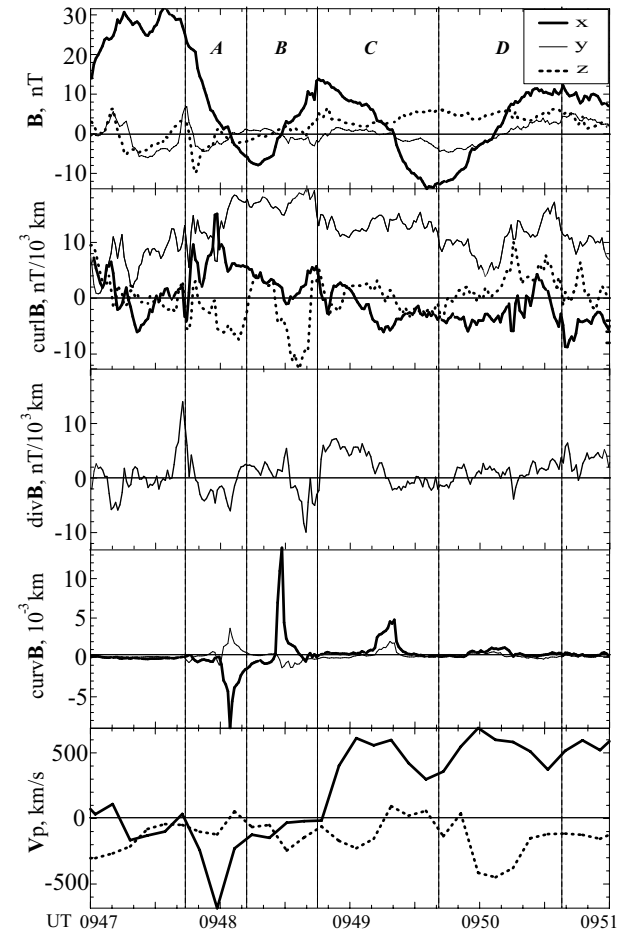


**Figure 2.** Cluster measurements at the tetrahedron barycentre. From top to bottom: components of the magnetic field, components of  $\text{curl } \mathbf{B}$  vector, the magnetic field divergence,  $X$  and  $Y$  components of the magnetic field curvature vector, and proton bulk velocity as a mean value of s/c 1, 3 and 4 measurements versus UT.

observations can be interpreted as the tailward passage of an X-line region over Cluster. The nonzero  $Y$  component of the magnetic curvature vector probably results from the tilt of the current sheet with respect to the  $Z_{GSM}=0$  plane. The  $Z$ -component of the curvature vector (not shown) is negligibly small.

CIS/CODIF onboard s/c 1, 3 and 4 detected tailward moving protons of energy 1-10 keV (s/c 1) and  $\sim 10$  keV (s/c 3 and 4) during crossing  $A$ , 0.1-1 keV for s/c 1, which stays at the level of  $B_x \sim 20$  nT, and  $\sim 1$  keV for s/c 3 and 4 during crossing  $B$ , and  $\geq 10$  keV during crossings  $C$  and  $D$  (not shown). These observations conform to ion flow in the vicinity of an X-line: cold (lobe) plasma inflow ( $B$ ) and accelerated plasma outflow ( $A$ ,  $C$ ,  $D$ ).

Using the calculated  $\text{curl } \mathbf{B}$ , we analyzed the current sheet structure near the X-line. Figure 3 shows the  $y$ -component of  $\text{curl } \mathbf{B}$ , which results mostly from the magnetic field gradient along  $Z_{GSM}$ , versus  $B_x$  in the tetrahedron barycentre ( $B_{xc}$ ). During crossing  $A$ , the  $Y$ -component of the current density associated with the tailward ion flow tends to decrease when  $B_{xc} \rightarrow 0$ . After jumping to a large value, which probably is a temporal effect,  $j_y \sim (\text{curl } \mathbf{B})_y$  has a local minimum near  $B_{xc} \sim 0-5$  nT in crossing  $B$  (Figure 3, thick curve, marked by bullets). It should be noted that the estimate of  $\text{curl } \mathbf{B}$  during the interval 0948:25-0948:35 UT, when s/c 2, 3, and 4 are in SH, and s/c 1 stays in NH, is of minimum accuracy. The linear estimate of the magnetic field divergence for this interval yields

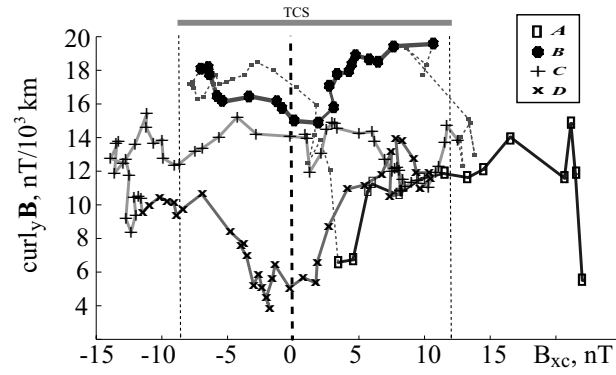


**Figure 3.** Current sheet structure in the vicinity of the X-line: the  $Y$ -component of  $\text{curl } \mathbf{B}$  (cross-tail current density) versus  $B_x$  in the tetrahedron barycentre.

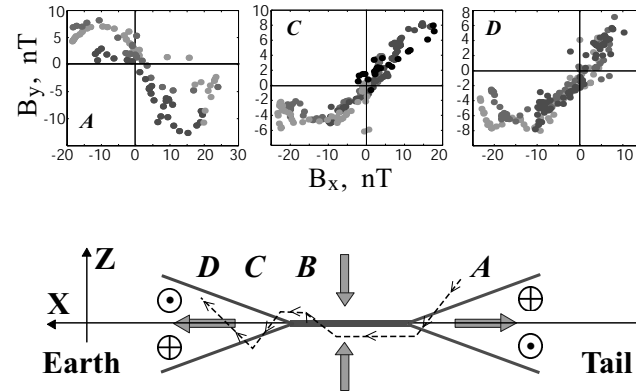


**Figure 4.** The out-of-plane Hall magnetic field component  $B_y$  versus  $B_x$  over neutral sheet crossings  $A$ ,  $C$  and  $D$  (upper panel), and a sketch of reconnected current sheet structure with Hall currents.  $\odot$  and  $\oplus$  denote the  $B_y$  direction; dotted line shows schematic representation of the Cluster barycentre trajectory.

absolute values of  $1-5$  nT/ $10^3$  km, an order of magnitude less than the estimate of  $\text{curl } \mathbf{B}_y$ , but comparable with the difference between the maximum and minimum values of  $j_y$  in crossing  $B$ . Thus, the current density during this interval has a rather flat distribution with a tendency to decrease when  $B_x \rightarrow 0$ .

The value of  $j_y$  drops to a smaller value between crossings  $B$  and  $C$  and exhibits a flat profile (curve marked by "+" sign) during crossing  $C$ . This is associated with earthward proton flow. In crossing  $D$  (curve marked by "x") the  $j_y$  profile has a pronounced minimum at  $B_{xc} \sim 0$ .

Figure 4 shows scatter plots of the out-of-plane  $B_y$  component versus  $B_x$  for crossings  $A$ ,  $C$  and  $D$ . During the NH $\rightarrow$ SH crossing  $A$ ,  $B_y$  changes from being positive at  $B_x > 0$  (NH) to negative at  $B_x < 0$  (SH). The crossings  $C$  (NH $\rightarrow$ SH) and  $D$  (NH $\rightarrow$ SH) are characterized by positive  $B_y$  at  $B_x > 0$  and negative  $B_y$  at  $B_x < 0$ . These results are consistent with the presence of Hall currents. A sketch of the reconnected current sheet structure including the Hall magnetic field near the X-line is given in the bottom panel of Figure 4.

To complete this overview of Cluster observation we note the behavior of the  $Z$ -component of the proton bulk velocity in crossing  $D$ . The large almost perpendicular to the magnetic field directed negative  $V_z \sim -500$  to  $-700$  km s $^{-1}$  was detected by Cluster 1, 3, 4 during the SH $\rightarrow$ NH crossing in combination with a large  $V_x$ . At the same time  $V_y$  is negative, mainly perpendicular to the magnetic field, and varies in the range  $-100 < V_y < -500$  km s $^{-1}$ . The proton flow thus forms a 3D vortex in the earthward outflow region.

### 3. Discussion

We interpret the Cluster observations of 1 October 2001 at 0947-0951 UT in terms of an X-line in tailward motion past the spacecraft. The Cluster four-point measurements allow us to calculate the magnetic field curvature and curl and to analyze the current sheet structure near the X-line. The actual value of the current density  $\mathbf{j} = \mu_0^{-1} \text{curl } \mathbf{B}$  may be underestimated because the inter-spacecraft separations are too large in order to detect any small-scale current structures.

The current sheet profiles in the crossings  $A$  and  $D$  are consistent with a bifurcated current structure in both reconnection outflow regions, as predicted by MHD/Hall-MHD and kinetic simulations of the reconnection process, as well as some analytical solutions. A double-peak current structure had already been detected in the distant tail by Hoshino *et al.* [1996] from the statistical analysis of Geotail measurements. It was interpreted there in terms of a pair of Petschek-type shock waves formed in localized reconnection. Asano [2001] showed that the cross-tail current has a bifurcated structure in the post-plasmoid plasma sheet in agreement with simulation results of Arzner and Scholer [2001]. Recently, Nakamura *et al.* [2002] Runov *et al.* [2002] and Sergeev *et al.* [2002] observed bifurcated current sheets in the Cluster observations. In contrast to this paper, in those cases the bifurcation could not be directly attributed to magnetic reconnection.

The thick curve, corresponding to crossing  $B$  in Figure 3 indicates that the current density in this crossing is higher than during the other crossings. This intense current is localized in the  $B_x$  interval  $-10$  nT  $< B_x < 12$  nT. From the gradient estimate one finds a rough value of  $\lambda \sim 500-600$  km for the half-width of the current, in agreement with the estimate obtained from the fit to a Harris-type model [Harris, 1962]. We may therefore conclude that the Cluster observations support that the reconnection region at 0947-0951 UT has the structure sketched in Figure 4 and exhibits two outflow regions that are bounded by bifurcated currents, and a comparably thin current sheet in the center. The TCS was observed by Cluster

during the 30 s long interval 0948:07-0948:40 UT. Referring to the average value of  $\langle V_x \rangle \approx 200 \text{ km s}^{-1}$  during this interval we get as an estimate of the length of the TCS along  $X$  a value of  $\sim 6000$ - $7000 \text{ km}$ , about 10 ion Larmor radii (calculated for 10-keV ions in a 20 nT field). It should be noted that the structure of the TCS differs from a Harris sheet. The current density profile has a local minimum at  $B_x \sim 0$ . Such a structure may result from some instability or the development of turbulence. It may also be the result of TCS-"aging" as has recently been described by Zelenyi *et al.* [2002].

The  $Y$ -component of the magnetic field has a quadrupolar spatial distribution. This behavior of  $B_y$  near the magnetic X-line is predicted by Hall-MHD, hybrid and kinetic simulations of the reconnection process and is indication for the magnetic X-line being detected [e.g., Nagai *et al.*, 2001]. The observations allow for an estimate of the ion inertial length  $d_i$ , using the calculated gradient of the magnetic field. One finds that  $d_i \sim 1742$ , 1451, and 2540 km for crossings  $A$ ,  $C$  and  $D$ , respectively.

#### 4. Concluding Remarks

Magnetic reconnection relies on microscopic aspects of magnetic field and particle dynamics. In the first place it is the dynamics of the electrons that determines the reconnection process [for a recent account see e.g. Sitnov *et al.*, 2002]. Decoupling of the electron motion from ions takes place on the ion inertial scale near the X-line. This decoupling gives rise to Hall currents and generates a Hall  $B_y$  field component. It thus can be detected in a comparably large volume, while the decoupling of the electrons from the magnetic field takes place on the electron inertial scale and thus usually escapes observation. One should, however, keep in mind that the Hall field is but an indication of decoupling of electron and ion dynamics. In the reconnection process itself it plays a little role as it merely rotates the total field. In this sense the characteristic ion and electron inertial lengths are the crucial parameters of the physical processes in the reconnection region. In our analysis of Cluster X-line observations on 1 October 2001, Cluster was able to resolve some of the fine structure of the reconnection region and to determine these scales. The accuracy of the estimates of characteristic lengths as well as the scales of the gradient and curl is still relatively low. It will be essentially higher with upcoming smaller inter-spacecraft separation. Nonetheless, for the event under consideration in this communication we were able to draw a consistent picture of the structure of the tail reconnection region in relation to currents, flows, and the geometry of the magnetic field.

**Acknowledgments.** We thank H.-U. Eichelberger, G. Laky, Y. Bogdanova for helping Cluster data analysis, and T. Terasawa, V. Sergeev, M. Sitnov, V. Semenov, T. Nagai, and M. Fujimoto for helpful discussion and comments. We acknowledge the CSDS and the World Data Center for Geomagnetism in Kyoto.

#### References

- Arzner, K., and M. Scholer, Kinetic structure of the post plasmoid plasma sheet during magnetic reconnection, *J. Geophys. Res.*, **106**, 3827, 2001.
- Asano, Y., Configuration of the thin current sheet in substorms, Ph.D. thesis, Univ. Tokyo, 2001.
- Balogh, A., et al., The Cluster magnetic field investigation: overview of in-flight performance and initial results, *Ann. Geophys.*, **19**, 1207, 2001.
- Chanteur, G., Spatial interpolation for four spacecraft: Theory, In *Analysis Methods for Multi-Spacecraft Data*, G. Paschmann and P. Daly (Eds.), ISSI Scientific Report SR-001, ISSI/ESA, 349 - 369, 1998.
- Harris, E.G., On a plasma sheet separating regions of oppositely directed magnetic field, *Nuovo Cimento*, **23**, 115, 1962.
- Hesse, M., J. Birn, and M. Kuznetsova, Collisionless magnetic reconnection: Electron processes and transport modeling, *J. Geophys. Res.*, **106**, 3721, 2001.
- Hoshino, M., A. Nishida, T. Mukai, Y. Saito, and T. Yamamoto, Structure of plasma sheet in magnetotail: Double-peaked electric current sheet, *J. Geophys. Res.*, **101**, 24,775, 1996.
- Lottermoser R.-F., and M. Scholer, Undriven magnetic reconnection in magnetohydrodynamics and Hall Magnetohydrodynamics, *J. Geophys. Res.*, **102**, 4875, 1997.
- Lottermoser R.-F., M. Scholer, and A. P. Matthews Ion kinetic effects in magnetic reconnection: Hybrid simulations, Hall Magnetohydrodynamics, *J. Geophys. Res.*, **103**, 4547, 1998.
- Nakamura, R. et al., Fast flow during current sheet thinning, *Geophys. Res. Lett.*, in press, 2002.
- Nakamura, M. S., M. Fujimoto, and K. Maezawa, Ion dynamics and resultant velocity space distributions in the course of magnetotail reconnection, *J. Geophys. Res.*, **103**, 4531, 1998.
- Nagai, T., I. Shinohara, M. Fujimoto, M. Hoshino, Y. Saito, S. Machida, and T. Mukai, Geotail observations of the Hall current system: Evidence of magnetic reconnection in the magnetotail, *J. Geophys. Res.*, **106**, 25,929, 2001.
- Øieroset, M., T. D. Phan, M. Fujimoto, R. P. Lin, and R. P. Lepping, *In situ* detection of collisionless reconnection in the Earth's magnetotail, *Nature*, **412**, 414, 2001.
- Pritchett, P.L., Geospace Environment Modeling magnetic reconnection challenge: Simulations with a full particle electromagnetic code, *J. Geophys. Res.*, **106**, 3783, 2001.
- Rème, H., et al., First multispacecraft ion measurements in and near the Earth's magnetosphere with the identical Cluster ion spectrometry (CIS) experiment, *Ann. Geophys.*, **19**, 1303, 2001.
- Runov, A., R. Nakamura, W. Baumjohann, T.L. Zhang, M. Volwerk, H.-U. Eichelberger, and A. Balogh, Cluster observation of a bifurcated current sheet, *Geophys. Res. Lett.*, submitted 2002.
- Sato, T. and T. Hayashi, Externally driven magnetic reconnection and a powerful magnetic energy converter, *Phys. Fluids*, **22**, 1189, 1979.
- Scholer, M., Undriven magnetic reconnection in an isolated current sheet, *J. Geophys. Res.*, **94**, 8805, 1989.
- Semenov, V. S., O. A. Drobysh, and M. F. Heyn, Analysis of time-dependent reconnection in compressible plasmas, *J. Geophys. Res.*, **103**, 11,863, 1998.
- Sergeev, V. A. et al., Current sheet flapping motion and structure observed by Cluster, *Geophys. Res. Lett.*, submitted 2002.
- Sitnov, M. I., A. S. Sharma, P. N. Guzdar, and P. H. Yoon, Reconnection onset in the tail of Earth's magnetosphere, *J. Geophys. Res.*, **107**, 1256, doi:10.1029/2001JA009148, 2002.
- Sonnerup, B. U. Ö., Magnetic field reconnection, In *Solar System Plasma Physics*, vol. III, ed. L. T. Lanzerotti, C. F. Kennel, and E. N. Parker, pp. 45-108, North-Holland, New York, 1979.
- Terasawa, T., Hall current effect on tearing mode instabilities, *Geophys. Res. Lett.*, **10**, 475, 1983.
- Ugai, M. and T. Tsuda, Magnetic field-line reconnection by localized enhancement of resistivity. Part 1. Evolution in a compressible MHD fluid, *J. Plasma Physics*, **17**, 337, 1977.
- Zelenyi, L., D.C. Delcourt, H.V. Malova, and A.S. Sharma, "Aging" of the magnetotail current sheets, *Geophys. Res. Lett.*, **29**(12), DOI 10.1029/2001GL013789, 2002.
- A. Runov Institut für Weltraumforschung der ÖAW, Schmiedlstr. 6, A-8042, Graz, Austria. (Andrei.Runov@oeaw.ac.at)

(Received \_\_\_\_\_.)